



## THERMAL ANALYSIS OF THE FASTRAC CHAMBER/NOZZLE

**Darrell Davis**  
Marshall Space Flight Center

### ABSTRACT

This paper will describe the thermal analysis techniques used to predict temperatures in the film-cooled ablative rocket nozzle used on the Fastrac 60K rocket engine. A model was developed that predicts char and pyrolysis depths, liner thermal gradients, and temperatures of the bondline between the overwrap and liner. Correlation of the model was accomplished by thermal analog tests performed at Southern Research, and specially instrumented hot fire tests at the Marshall Space Flight Center. Infrared thermography was instrumental in defining nozzle hot wall surface temperatures. In-depth and outboard thermocouple data was used to correlate the kinetic decomposition routine used to predict char and pyrolysis depths. These depths were anchored with measured char and pyrolysis depths from cross-sectioned hot-fire nozzles. For the X-34 flight analysis, the model includes the ablative Thermal Protection System (TPS) material that protects the overwrap from the recirculating plume. Results from model correlation, hot-fire testing, and flight predictions will be discussed.

### INTRODUCTION

The Fastrac program provides a low-cost, 60,000 lb (60K) thrust, rocket engine to the aerospace community. Part of this low-cost design is an ablative chamber/nozzle assembly that is actively film-cooled with RP1. The chamber/nozzle is designed for one time use only and will be replaced after every flight. The baseline chamber/nozzle consists of a tape-wrapped silica phenolic liner with a filament-wound carbon epoxy overwrap added for extra strength. A filament wound glass phenolic overwrap is also being tested as part of a parallel verification effort. The flight nozzles will have a 30:1 area ratio. However, most of the nozzles that have been ground tested have a 15:1 area ratio since the 30:1 nozzle is underexpanded at sea level.

The concerns during the design phase included: effects of the film cooling, degree of surface recession and the ability to maintain the liner to overwrap bondline below 300 F. The insulative properties of the silica phenolic protect the bondline during firing (typically 150 seconds), however the "soakback" effect causes the bondline to exceed the limit after shutdown and to potentially create a debond. The soakback effect was mentioned as a design problem at the Preliminary Design Review. To address this, as well as the other desing concerns, extra tests were added to the test plan to assist in gathering data to refine the thermal model. As the design progressed, it was obvious that the liner had to be thicker to protect the bondline. This was an undesirable solution since it increased the weight of the nozzle. The solution was to thicken the liner as much as possible only at the attach rings and add to shear pins to distribute the load into the nozzle in case the rings still came loose. This resulted in the baseline configuration shown in Figure 1. Table 1 presents the design thicknesses at key locations.

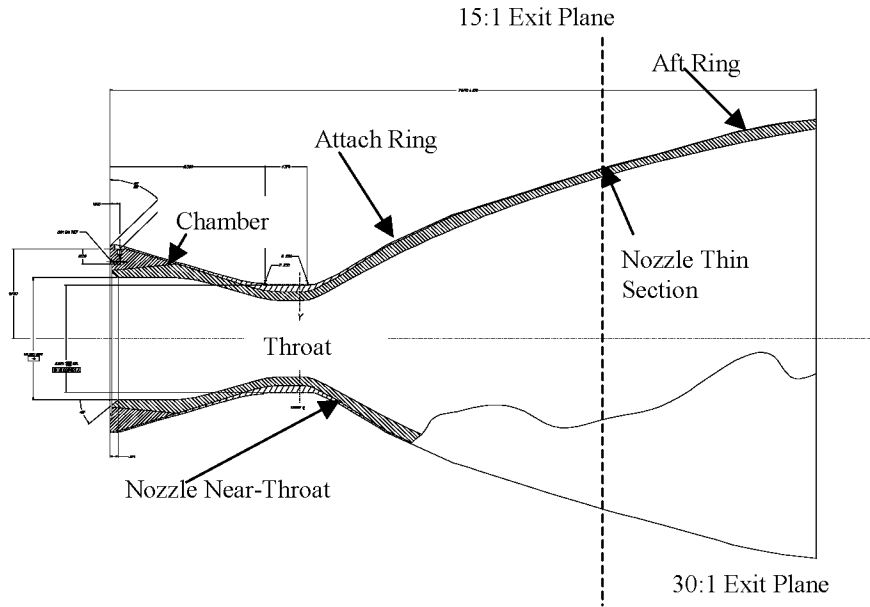


Figure 1: Fastrac Chamber/Nozzle Baseline Configuration.

	Silica Phenolic Thickness	Graphite Epoxy Thickness
Chamber	0.987	0.253
Throat	0.850	0.807
Nozzle Near-Throat	0.852	0.316
Attach Ring	1.349	0.123
Nozzle Thin Section	0.801	0.072
Aft Ring	1.194	0.062

Table 1: Fastrac Chamber/Nozzle Design Thickness.

## MODEL DESCRIPTION

A one-dimensional SINDA model was developed to predict in-depth temperature response and bondline temperatures for ground tests and for flight conditions. The SINDA model consisted of 45 finite element nodes across the thickness of the silica phenolic liner and 5 nodes through the graphite epoxy overwrap. A non-linear grid was used to capture the high gradients near the surface while minimizing the overall number of nodes. Material properties for the virgin and charred silica phenolic were obtained through testing at Southern Research, Inc. (SORI) in Birmingham, AL. Preliminary hot gas temperature predictions were provided by the CFD group at the Marshall Space Flight Center. SINDA/CMA<sup>1</sup>, a kinetic decomposition routine, based on the Arrhenius equation, was added to account for the effect of material decomposition and pyrolysis gas formation. Cork was added to the external nozzle surfaces to protect the graphite epoxy from the plume recirculation environments during flight. ABL<sup>2</sup>, an in-house developed code that can be coupled with SINDA, was used to size the cork. ABL uses an empirically derived recession rate versus heat rate curve to calculate surface recession of the cork while tracking thermal capacitance and conduction path lengths to calculate heat transfer through the receding material. This is the first model generated at MSFC that has incorporated SINDA/CMA and ABL to account for material decomposition of two different materials experiencing two different environments.

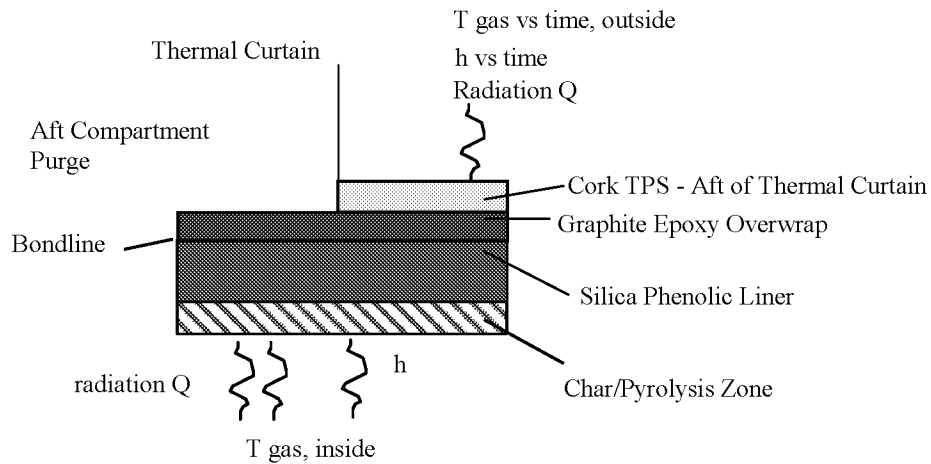


Figure 2: Schematic Representation of SINDA Model

## TESTING

Preliminary material testing was performed at MSFC's Improved Hot Gas Facility (IHGF) and Wright Patterson Air Force Base's Laser Hardened Material Evaluation Laboratory (LHMEL). These tests did not provide much data that could be used to validate the in-depth model predictions, however they verified the assumption that the surface would not recede at the expected hot-fire conditions. The first data used to correlate the model came from Thermal Analog tests performed at SORI<sup>3</sup>. The test provided one-dimensional heating of a 2.0" x 2.0" x 0.85" coupon of silica phenolic/graphite epoxy lay-up by exposing the coupon surface to a resistively heated graphite heater. The coupon surface was heated at rates that simulated actual engine firings. A schematic of the basic facility is shown in Figure 3.

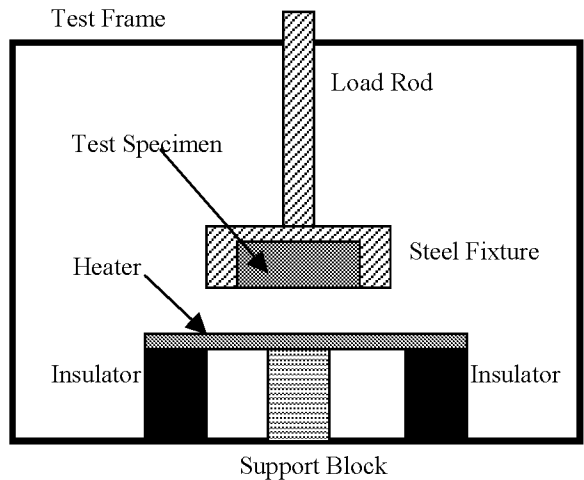


Figure 3: Schematic of SORI Analog Tests

A total of three samples were tested. The first two tests runs were for 150 seconds and the third was for 230 seconds. Temperature of the surface, backside, and five in-depth locations were recorded with thermocouples. Depths of the imbedded thermocouples were determined by CT techniques. The recorded surface temperature was used as an input to the SINDA model and temperatures were predicted at the measured thermocouple depths. Because of uncertainty in the char properties, and the unknown material properties in the pyrolysis region, material properties were adjusted until the SINDA model results matched the results from the Thermal Analog Tests. Char and heat-affected depths were also taken from these samples. This data was used to anchor the kinetic decomposition routine.

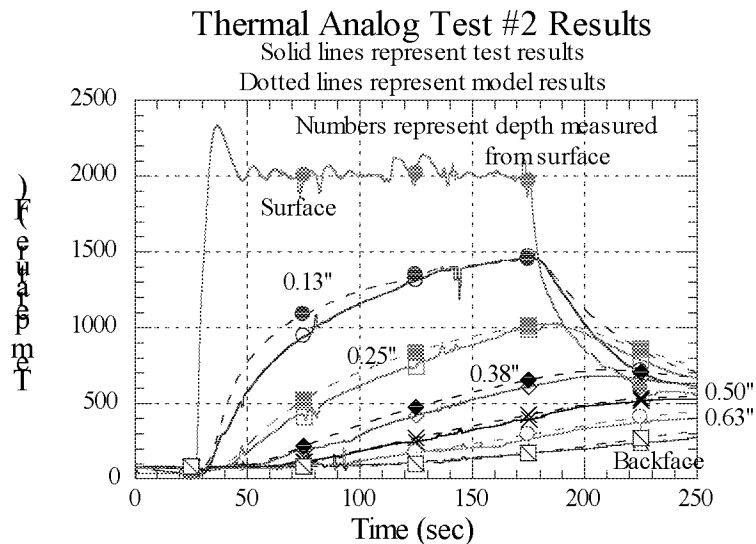


Figure 4: Model Comparison to SORI Analog Tests

A significant amount of data was gathered from hot fire component testing performed at MSFC's Test Stand 116. These were static tests to verify the design of the Thrust Chamber Assembly (TCA). The propellants were pressure-fed instead of using the actual Fastrac turbomachinery. During this series of tests, an attempt was made to gather as much data as resources would allow. This data would prove valuable to the validation of the thermal math model.

All static tests had two thermocouples installed in holes drilled through the aft-facing surface of the silica phenolic. One was a bare Type C thermocouple mounted flush with the liner surface to measure surface temperature, the other was a shielded Type C thermocouple mounted with the bead about 0.125" into the flow to measure the local hot gas temperature. An infrared scanner was also used to determine the interior surface temperature. The results from these two methods matched well and enabled the surface temperatures used in the model to be lowered.

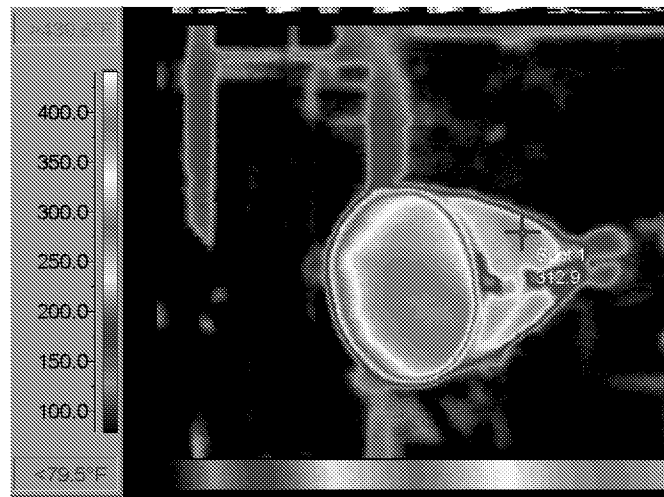


Figure 5: Infrared Image of Fastrac Nozzle Showing Soakback Effect

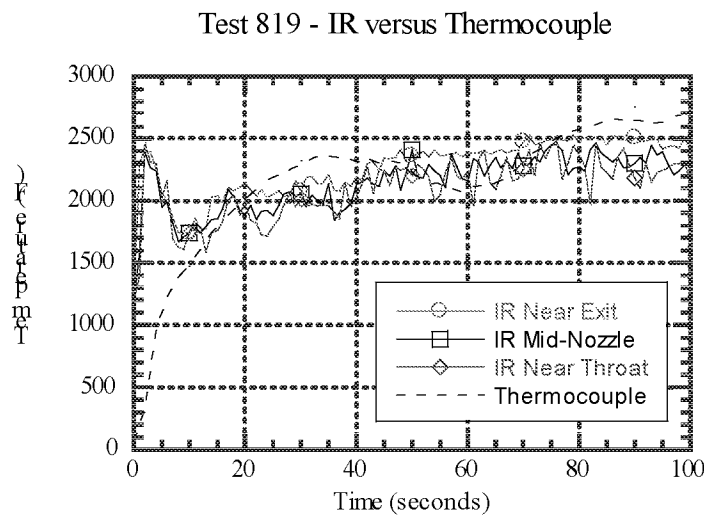


Figure 6: Comparison of Temperatures from Thermocouples and Infrared

In two of the early tests, designated 60K #1 and 60K #2, thermocouple plugs were used to measure in-depth temperature response. This process was developed during earlier technology development programs at MSFC. The plugs were 0.25" silica phenolic cylinders into which were imbedded three thermocouples.

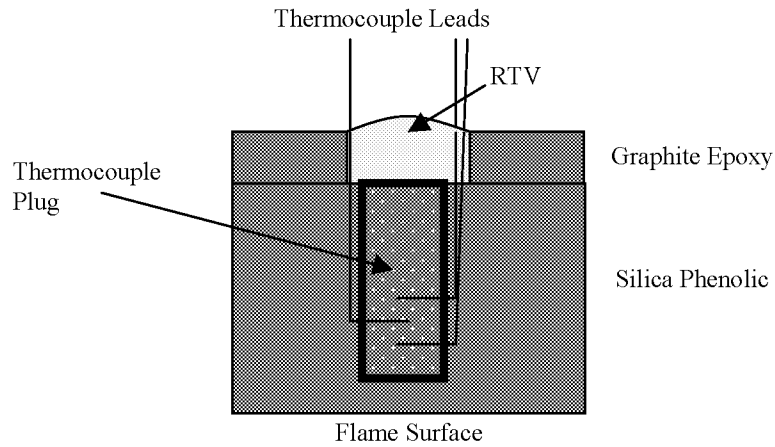


Figure7: Schematic of Thermocouple Plug

The plugs were laid up in the same manner as the liner material. Care had to be taken during installation to ensure proper placement of the thermocouple leads within the plug. A hole was drilled into the silica phenolic liner from the backside to within a nominal 0.100" from the surface and the plugs were installed into these holes. Plugs were placed at four axial locations and two radial locations for each axial location.

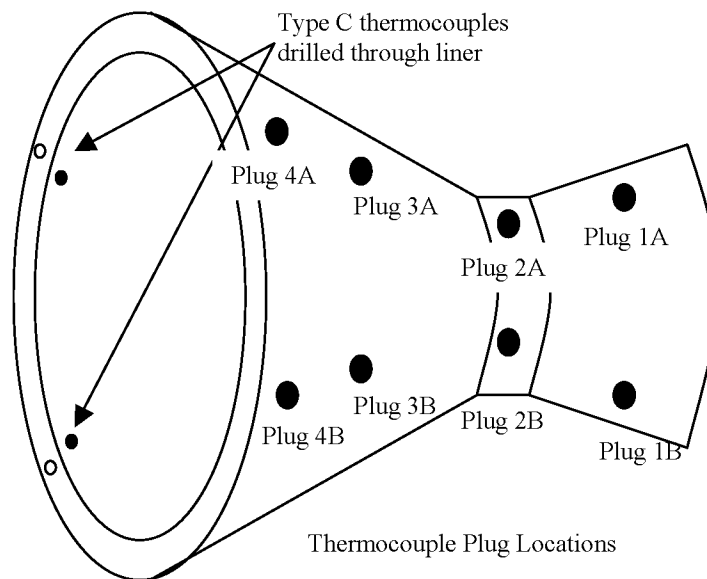


Figure8: Thermocouple locations on 60K #1 and 60k #2

All of the thermocouples in the A plugs were Type S while the B plugs used a combination of Type K and Type S. Because of the low conductivity of the silica phenolic, a steep thermal gradient exists in the liner and it was necessary to know the exact depths of the thermocouples. Depths of these thermocouples were again obtained by using CT techniques. However, the Type K thermocouples were invisible to CT. The Type K thermocouple data also tended to have more noise in the data and tended to open during the firing. Therefore the data from the Type S thermocouples in the A plugs was used in model verification. In the 60K #1 test, two Type S thermocouples failed, and during the 60K #2 test, a leak path developed around plug 2A and invalidated the thermocouple readings from that plug. Both tests were planned 150 second duration tests, however due to test anomalies, 60K #1 ran for 28 seconds and 60K #2 ran for 130 seconds. Thermocouple measurements versus model predictions are presented in the figures below

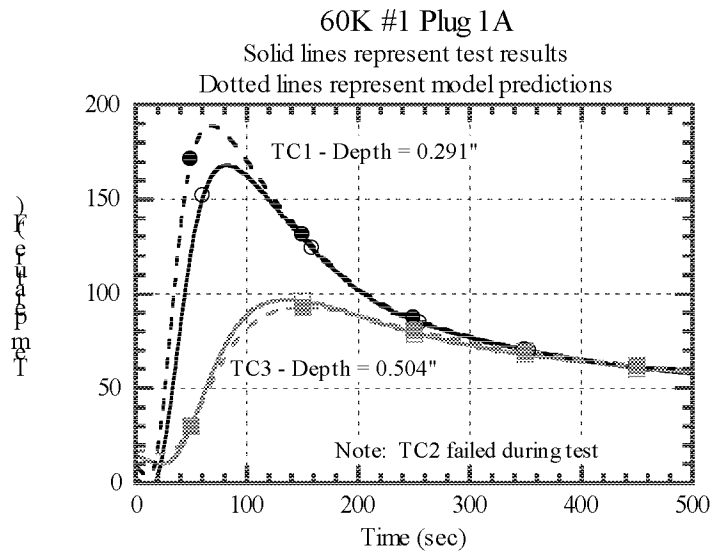


Figure 9: Model versus Test Data for Test 60K #1, Plug 1A

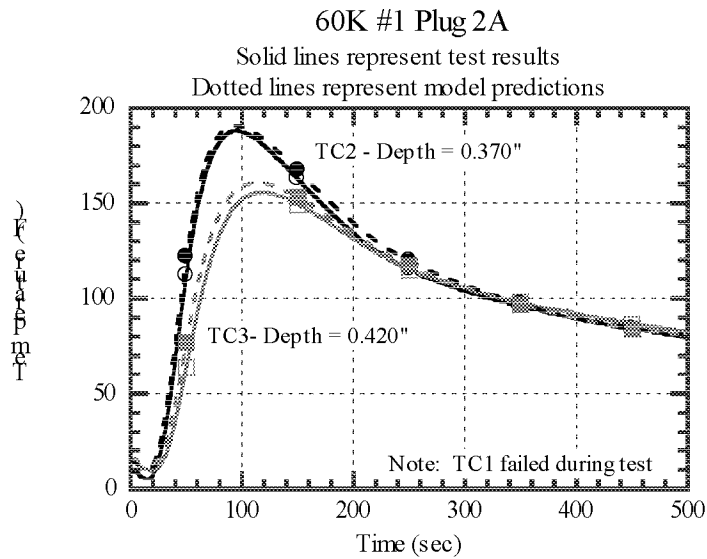


Figure 10: Model versus Test Data for Test 60K #1, Plug 2A

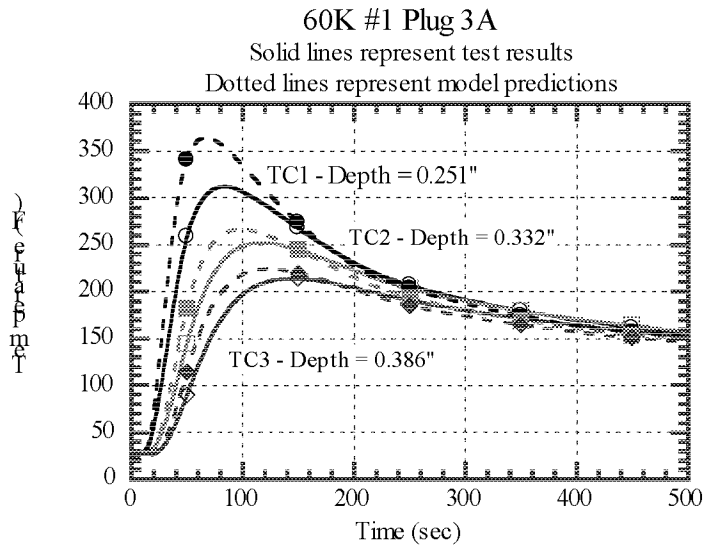


Figure 11: Model versus Test Data for Test 60K #1, Plug 3A

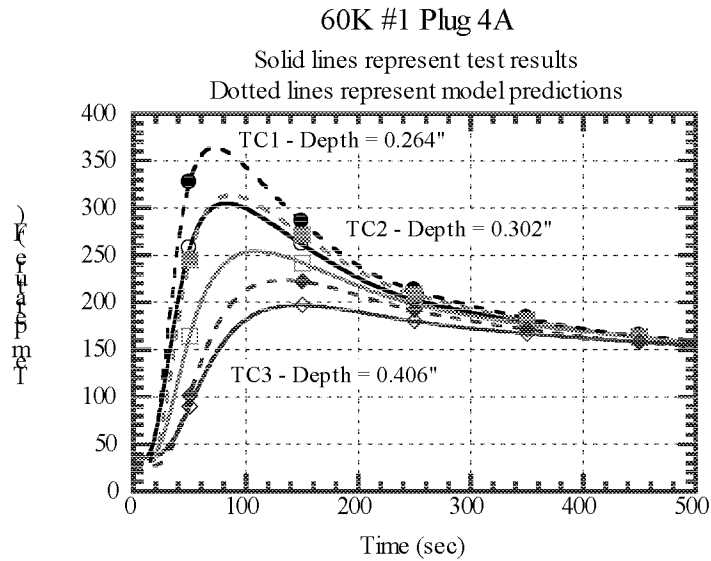


Figure 12: Model versus Test Data for Test 60K #1, Plug 4A

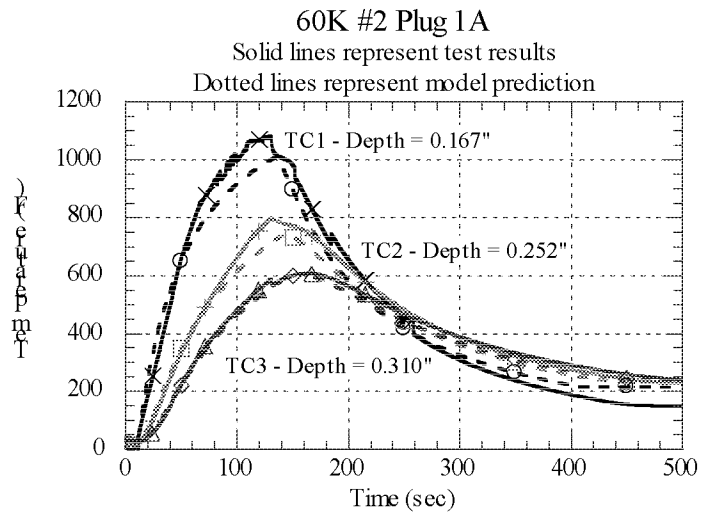


Figure 13: Model versus Test Data for Test 60K #2, Plug 1A

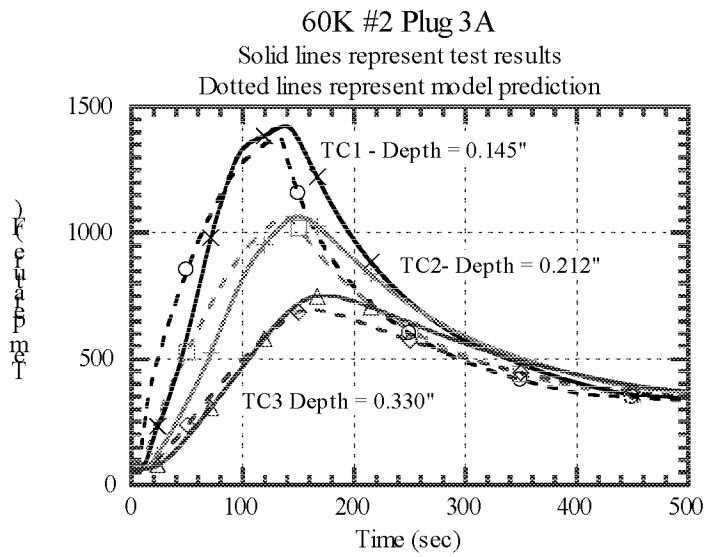


Figure 14: Model versus Test Data for Test 60K #2, Plug 3A

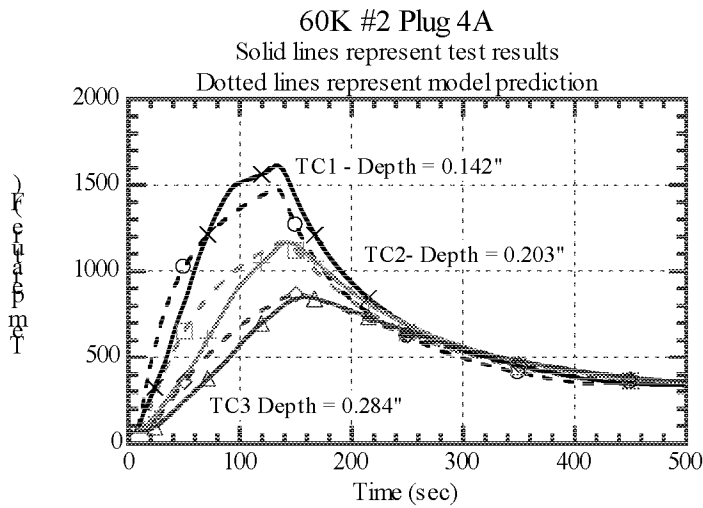


Figure 15: Model versus Test Data for Test 60K #2, Plug 4A

The 60K #1 and 60K #2 nozzles were sliced axially and post-test char and heat-affected depths were measured. Data from these tests also confirmed that there was no surface recession of the silica phenolic even during a 130-second test.

Since multiple short-duration tests were to be performed on each nozzle, the model was relied upon to verify that the bondline had not exceeded its temperature limit, and could be tested again. Therefore all static tests also had exterior thermocouples placed at key axial locations. These thermocouples provided data to anchor the model for each test and ensured reliable bondline predictions.

The next series of tests performed on the Fastrac nozzle occurred at the Stennis Space Center (SSC) in Pascagoula, Mississippi. These tests were system level validation tests that incorporated the turbomachinery with the TCA. Since drilling was not allowed on these nozzles, and the test stand does not provide adequate placement for the infrared scanner, external thermocouples are the only source of data on the tests at SSC.

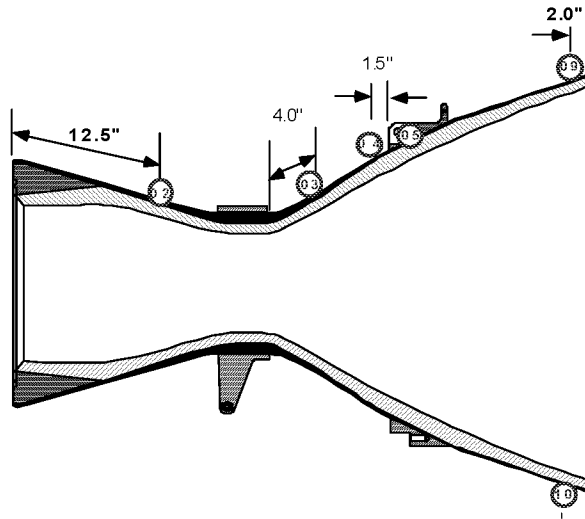


Figure 16: Thermocouple Placement on the H2 Series Tests at SSC

The H2 series tests were performed on a 15:1 nozzle with a glass phenolic overwrap. Results from thermal analysis and test data showed that the glass phenolic and graphite epoxy overwraps would perform very similarly thermally. Test H2A-2B and Test H2B-2 both ran for the planned full duration of 24 and 155 second, respectively. Comparison of model results with exterior thermocouple data is presented in the figures below. The model predictions tend to agree well with the thermocouple data. Most of the disagreements are caused by purges on the test stand cooling the nozzle surface after shutdown. While the model can account for this effect, the timeline and temperatures of these purges are not easily obtained.

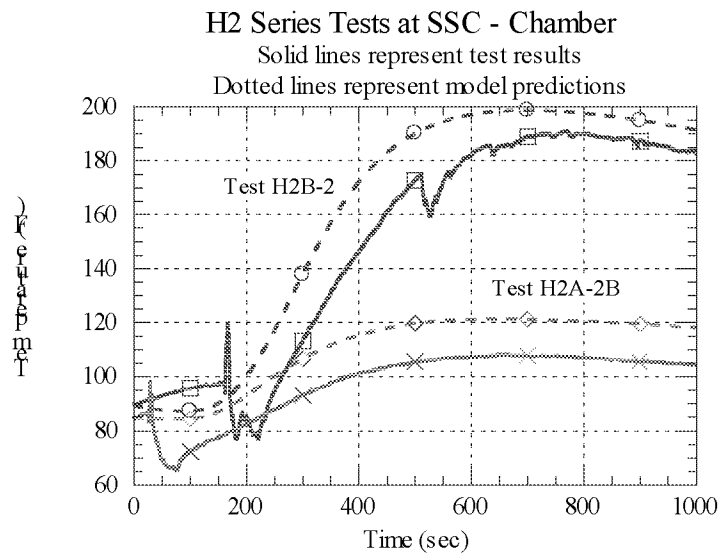


Figure 17: Fastrac Chamber Model Results versus Test Data for H2 Series Testing

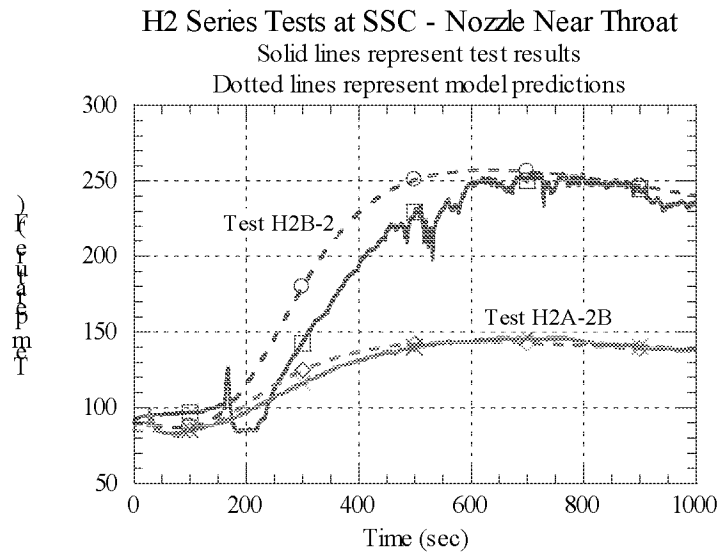


Figure 18: Fastrac Nozzle Near-Throat Model Results versus Test Data for H2 Series Testing

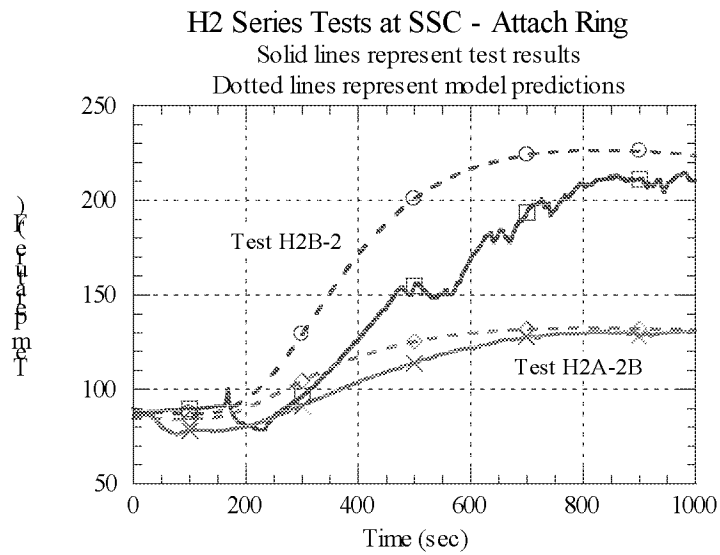


Figure 19: Fastrac Attach Ring Model Results versus Test Data for H2 Series Testing

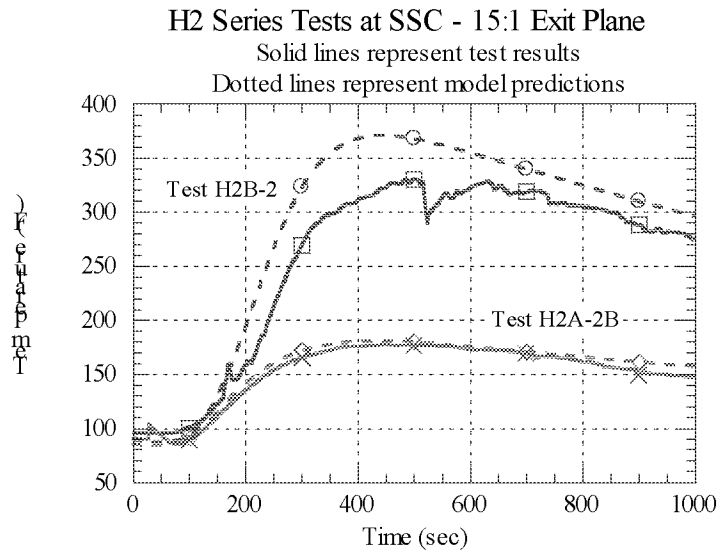


Figure 20: Fastrac Exit Plane Model Results versus Test Data for H2 Series Testing

These nozzles are also instrumented with strain gauges to allow structural analysts to verify their models. Data from these strain gauges can show where a debond has occurred. Figure 19 shows strain gauge and thermocouple data plotted together at the exit plane, where a visual examination confirmed a debond.

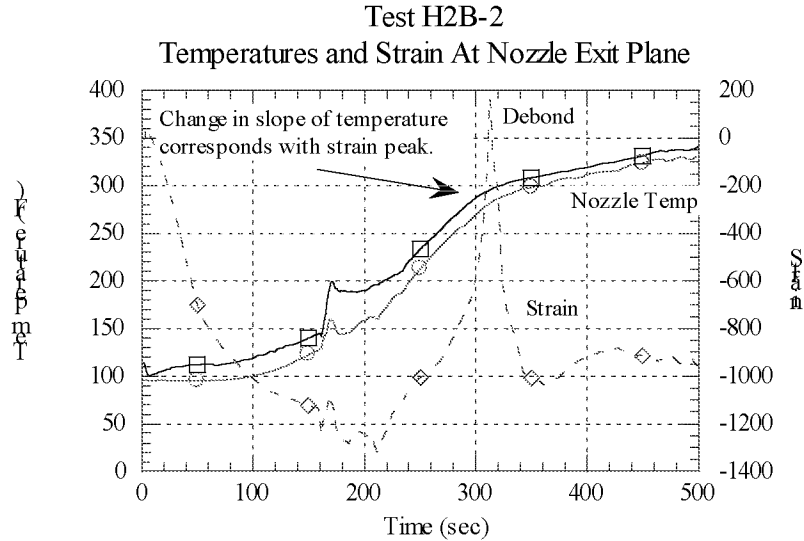


Figure 21: Thermocouple and Strain Gauge Data From Test H2B-2

The spike in the strain gauge data indicates a debond occurred at that time. At the same time, the thermocouple data changes slope. This is also an indication of a debond. When the graphite epoxy overwrap debonds from the liner, the conduction path from the liner to overwrap is broken. The overwrap is then more heavily influenced by convective cooling from the ambient temperature than by the radiant heating now produced by the liner. This causes a change in slope in the thermocouple response.

The nozzle near-throat region is an area of concern for potential debonding. In this section, the overwrap is becoming thinner due to an increase in local area ratio and the liner is not as thick as it is further downstream at the attach ring. Visual observations cannot reveal a debond in this region, and on-pad non-destructive evaluation (NDE) methods have not been developed to a point where they are feasible to use in small, tight spaces. Strain gauge data from the near-throat region of Test H2B-2 seems to indicate a debond. When the thermocouple data is plotted alongside the strain gauge data, Figure 20, it may also show indications of a debond by the change of slope in the temperature trace.

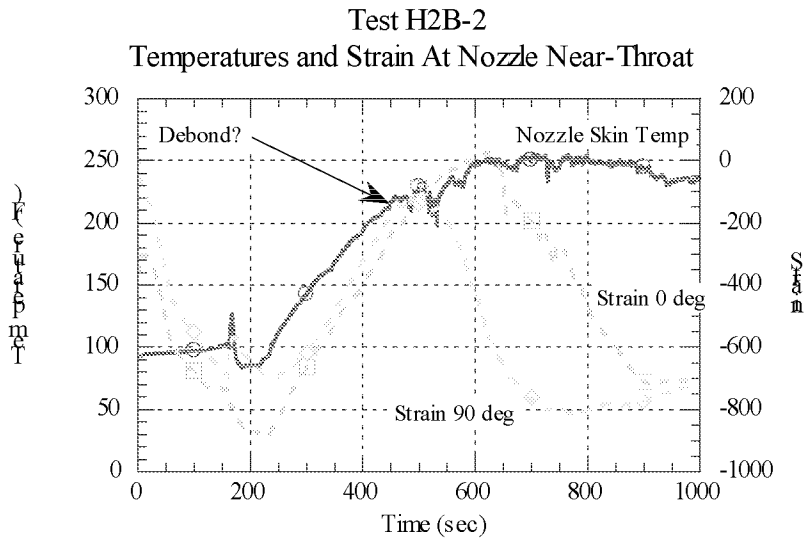


Figure 22: Thermocouple and Strain Gauge Data from Test H2B-2

Post test laboratory NDE could not positively declare a debond at this location, but did reveal a low-density area. It is possible that this configuration of thermocouples and strain gauges could be used for health monitoring of the nozzle during ground tests.

### THERMAL PREDICTIONS FOR STRUCTURAL ANALYSIS

Once the model had been proven reliable and able to match test results, it was used to provide two-dimensional thermal distributions to structural analysts. The kinetic decomposition routine could not be adapted to a two-dimensional grid. Since there was very little difference in local plume temperatures and therefore no  $\Delta T$  to drive axial conduction, it was determined that an interpolation of 1-D results would provide the necessary data. The analytical nozzle was separated into 28 1-D slices as shown in Figure 21.

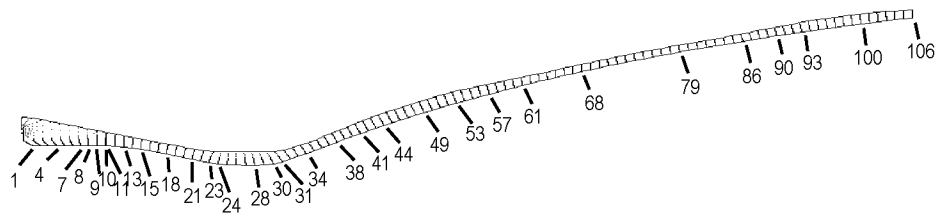


Figure 23: Locations of 1-D Slices Used to Generate 2-D Thermal Distributions

Each slice was run with its corresponding gas temperature, heat transfer coefficient, silica phenolic thickness, graphite epoxy thickness to provide a thermal gradient profile at that location. The results were interpolated onto a 2-D PATRAN finite element mesh. Results provided for structural analysis included hot and cold extremes for both ground and flight.

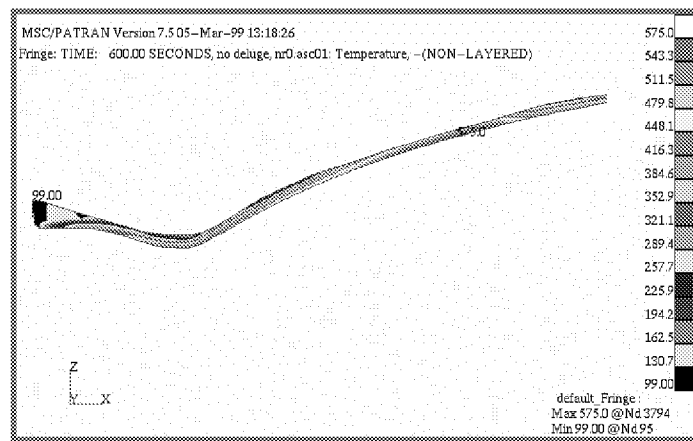


Figure 24: Example of Two-Dimensional Thermal Distribution

## FLIGHT PREDICTIONS

During flight, the overwrap forward of the heat shield will be exposed to environments generated inside the aft compartment. The nozzle itself will contribute to this environment, especially post-firing. Flight exterior nozzle temperatures were provided to Orbital Sciences Corporation for inclusion to their aft compartment model. Aft of the heat shield, the nozzle will be exposed to recirculation of the plume. MSFC's CFD group provided plume recirculation environments. ABL, an in-house code that runs concurrently with SINDA, was used to size the thermal protection system (TPS) materials. Two materials were selected for analysis; cork, Marshall Convergent Coating (MCC-1). MCC-1 is a sprayable ablator developed at MSFC containing cork, glass ecospheres and an epoxy resin. It is currently used as the main acreage TPS on the Solid Rocket Boosters. Results from the analysis showed that 0.25" of either material would protect the graphite epoxy overwrap to 300 F. Since MCC-1 is sprayable, it requires the

programming of a computer to follow the specific geometry of the nozzle. This made the MCC-1 more expensive for a short production run, so the program decided to use cork as the external TPS material. RT-455, a K5NA substitute, will be used as a closeout material and the entire TPS system will be covered with Acrymax paint.

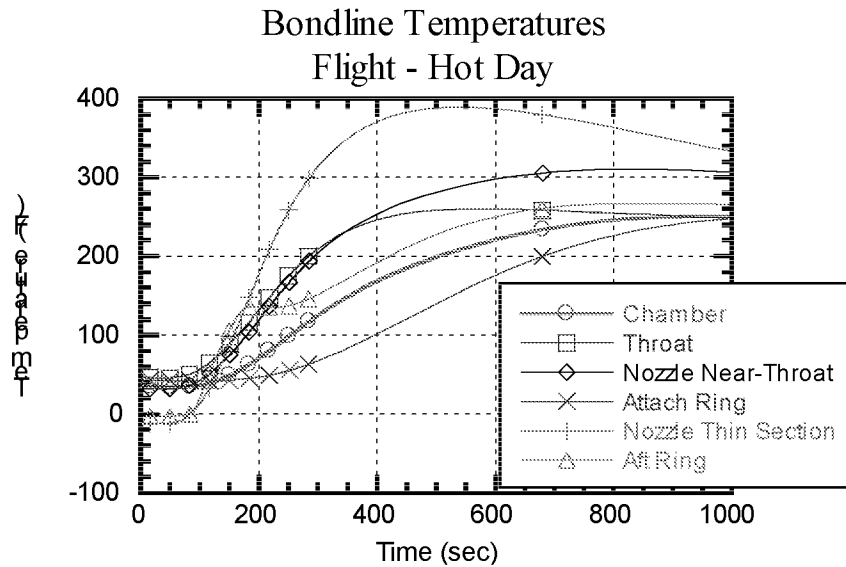


Figure 25: Flight Predictions

## CONCLUSIONS

Because of an extensive test program that generated data used to correlate the model, the model can be trusted to give reliable results. These results indicate that during a 150-second engine burn, all bondlines will remain below 150F. However, this bondline limit will be violated during the soakback and will potentially cause a debond.

## ACKNOWLEDGEMENTS

The author wishes to acknowledge the contributions of Louie Clayton for help with the SINDA/CMA routine, Donald Bryan for help with the infrared imaging, and Bruce Tiller for guidance.

## REFERENCES

1. "SINDA Temperature and Pressure Predictions of Carbon-Phenolic in a Solid Rocket Motor Nozzle Environment", 1992 JANNAF Conference, Moffat Field, Palo Alto, CA, J. Louie Clayton
2. "SINDA/ABL Solution Routine Updates", J. Louie Clayton, NASA Internal Memorandum, ED63(25-96), 1996

3. "Thermal Analog Testing of Fastrac MX2600 Silica Phenolic, Final Report to MSFC", Michael D. Johns, SRI-ENG-98-26-8657.15, 1998